P14R.1 ON THE EQUIVALENCE OF THE DUAL-WAVELENGTH AND POLARIMETRIC EQUATIONS FOR ESTIMATION OF THE RAINDROP SIZE DISTRIBUTION

Robert Meneghini[1] and Liang Liao[2]

[1]Code 614.6, NASA/GSFC, Greenbelt, MD 20771
[2]Goddard Earth Science and Technology Center/ Caelum Research Corp., Rockville, MD 20850

1. INTRODUCTION

In writing the integral equations for the median mass diameter and number concentration, or comparable parameters of the raindrop size distribution, it is apparent that the form of the equations for polarimetric and dual-wavelength radars are identical when attenuation effects are included. The differential backscattering and extinction coefficients appear in both sets of equations: for the polarimetric equations, the differences are taken with respect polarization at a fixed frequency while for the dual-wavelength equations, the differences are taken with respect to frequency at a fixed polarization.

The similarity also extends to the way these equations are solved. The forward recursion procedure tends to be unstable as the attenuation out to the range of interest becomes 'large' in some sense. This is analogous to the case of a single attenuating-wavelength radar where the forward solution to the Hitschfeld-Bordan [Hitschfeld and Bordan, 1954] equation becomes unstable as the attenuation increases. To circumvent this problem, the equations can be expressed in the form of a final-value problem so that the recursion begins at the far range gate and proceeds inward towards the radar.

Solving the problem in this way traditionally requires estimates of path attenuation to the final gate: in the case of orthogonal linear polarizations, the attenuations at horizontal and vertical polarizations (same frequency) are required while in the dual-wavelength case, attenuations at the two frequencies (same polarization) are required.

As an alternative to using the constrained version of the equations, Mardiana et al. [2004], have shown that the backward integral equations can be solved in many cases by an iterative procedure. In this approach independent estimates of path attenuation are not needed.

An objective of the paper is to begin to make clear the relationships between the polarimetric and dual-wavelength equations so that they can be treated in a common theoretical framework. A second objective is to study the robustness of the solutions when constraints are available and when they are not. We begin by writing the integral equations for the median mass diameter, D_0, and number concentration, N_t, for the polarimetric and dual-wavelength radar returns. Simulations of the retrieval are presented for the case of an X-band polarimetric radar. In the final section of the paper, we discuss the relationship of the integral equation approach to an established method for attenuation correction of polarimetric data.

2. INTEGRAL EQUATIONS

The integral equations can be written in a relatively simple form but at the expense of requiring a number of definitions. The measured radar reflectivity factor at range r and frequency f, when the transmit and receive polarization are along the direction p, can be defined in terms of the radar return power by

$$Z_{m,pp}(r,f) = P_{r,pp}(r,f)r^2 /(C_{pp}(f)\left|K_w(f)\right|^2) \quad (1)$$

where C is the radar constant and $|K_w|^2$ is the dielectric factor of water which, by convention, is taken to be equal to its approximate value (0.93) for frequencies between 3 GHz and 10 GHz and for temperatures between 0 C and 20 C. The non-attenuated effective radar reflectivity factor, or simply radar reflectivity factor, Z, is related to Z_m by:

$$Z_{pp}(r,f) = Z_{m,pp}(r,f)\times \exp\{c\int_0^r [k_{r,pp}(s,f)+k_c(s,f)+k_v(s,f)]ds\} \quad (2)$$

where k_r, k_c, and k_v are the specific attenuations from precipitation, cloud water, and water vapor respectively, and where the precipitation may include rain, snow and mixed-phase hydrometeors. Throughout the paper, the co-polarized return powers are denoted by the subscripts pp where $pp = \{hh, vv\}$. Since the cloud and water vapor attenuation are polarization independent, we omit subscripts on these quantities. The units of k are taken to be dB km^{-1} so that $c = 0.2\ln(10) = 0.46$.

Defining

$$\tilde{Z}_{m,pp}(r,f) = 10\log_{10} Z_{m,pp}(r,f)$$
$$\tilde{Z}_{pp}(r,f) = 10\log_{10} Z_{pp}(r,f) \quad (3)$$

(2) can be written

$$\widetilde{Z}_{m,pp}(r,f) = \widetilde{Z}_{pp}(r,f) - A_{pp}(0,r;f) = \\ = \widetilde{Z}_{pp}(r,f) - (A_{pp}(0,r_n;f) - A_{pp}(r,r_n;f)) \quad (4)$$

where the two-way path attenuation from r_1 to r_2 is:

$$A_{pp}(r_1,r_2;f) = 2\int_{r_1}^{r_2}[k_{r,pp}(s,f) + k_c(s,f) + k_v(s,f)]ds \\ \equiv A_{r,pp}(r_1,r_2;f) + A_c(r_1,r_2;f) + A_v(r_1,r_2;f) \quad (5)$$

In the equations below, the notation $A_{pp}(0,r;f) = A_{pp}(r,f)$ is used. Next, the raindrop diameter distribution, $N(D,s)$ [m^{-3} mm^{-1}] is expressed as the product of the particle number concentration, N_t (m^{-3}), and a normalized size distribution, $n(D)$ (mm^{-1}):

$$N(D) = N_t n(D) \quad (6)$$

where, for the Gamma distribution,

$$n(D;\mu,\Lambda) = [\Lambda^{(\mu+1)} D^{\mu} / \Gamma(\mu+1)]\exp[-\Lambda D] \quad (7)$$

In general, Λ, μ are functions of the radar range. In the numerical results presented later, we use the median mass diameter, D_0 (mm), related to Λ, μ by

$$\Lambda D_0 = 3.67 + \mu \quad (8)$$

Finally, we introduce the backscattering and extinction integrals that are independent of N_t:

$$I_{b,pp}(r,f;D_0,\mu) = 10\log_{10}[c_Z\int_0^{\infty}\sigma_{b,pp}(f,D)n(r,D;D_0,\mu)dD] \quad (9)$$

$$I_{e,pp}(r,f;D_0,\mu) = c_e\int_0^{\infty}\sigma_{e,pp}(f,D)n(r,D;D_0,\mu)dD] \quad (10)$$

where $c_Z = {c_0}^4/(f^4\pi^5|K_w|^2)$ and $c_e = 4.343\times10^{-3}$, where c_0 is the speed of light. Note also that $k_{r,pp} = N_t I_{e,pp}$ and $\widetilde{Z}_{pp} = I_{b,pp} + 10\log_{10} N_t$.

Integral equations for D_0 and N_t for the dual-polarization case are obtained by writing $\widetilde{Z}_{m,pp}(r,f)$ and $\widetilde{Z}_{m,hh}(r,f) - \widetilde{Z}_{m,vv}(r,f)$ in terms of D_0 and N_t and expressing the path attenuation to range r in the form [Meneghini et al., 1992]:

$$A_{pp}(r,f) = A_{pp}(r_n,f) - A_{pp}(r,r_n;f) = \\ = A_{pp}(r_n,f) - 2\int_r^{r_n} N_t(s)I_{e,pp}(s)ds \quad (11)$$

Note that the path-integrated attenuation, PIA, is identified with the term $A_{pp}(r_n, f)$, where the path is terminated at the n^{th} gate. In (11), the attenuation from r to r_n is written in terms of the DSD parameters at the range gates within this range interval. This is the essence of the integral equation approach, where path attenuation to range r is found from an estimate of the total path attenuation and the DSD parameters in the range from r to r_n. The equations can be written in the following form:

$$I_{b,hh}(r) - I_{b,vv}(r) = (\widetilde{Z}_{m,hh}(r) - \widetilde{Z}_{m,vv}(r)) + \\ + (A_{hh}(r_n) - A_{vv}(r_n)) - 2\int_r^{r_n} N_t(s)[I_{e,hh}(s) - I_{e,vv}(s)]ds \quad (12)$$

$$\widetilde{N}_t(r) = \widetilde{Z}_m(r) - I_b(r) + A_r(r_n) - \\ - 2\int_r^{r_n} N_t(s)I_e(s)ds + A_c(r) + A_v(r) \quad (13)$$

$$\widetilde{N}_t \equiv 10\log_{10} N_t \quad (14)$$

For the dual-wavelength case, (13) remains the same but (12) is replaced with:

$$I_b(r,f_1) - I_b(r,f_2) = (\widetilde{Z}_m(r,f_1) - \widetilde{Z}_m(r,f_2)) + \\ + (A_r(r_n,f_1) - A_r(r_n,f_2)) - 2\int_r^{r_n} N_t(s)[I_e(s,f_1) - I_e(s,f_2)]ds + \\ + (A_c(r,f_1) - A_c(r,f_2)) + (A_v(r,f_1) - A_v(r,f_2)) \quad (15)$$

Note that the last four terms on the right-hand side of (15) are absent in (12). The difference arises from the fact that cloud and water vapor attenuation are frequency dependent but polarization independent. Note also that we have used the convention of suppressing the polarimetric (or frequency) dependence if all quantities in the equation are at the same polarization (or frequency). For example, in (12) all quantities are at the same frequency while in (15) all quantities are at the

same polarization; in (13) all quantities are measured or evaluated at the same frequency and polarization.

Eqs. (12)-(15) can be written in a form that makes explicit the unknown parameters of the drop size distribution and includes both dual-frequency and dual-polarization cases:

$$g_1(r;D_0,\mu) = h_1(r,r_n) - 2\int_r^{r_n} N_t(s) f_1(s;D_0,\mu) ds \tag{16}$$

$$g_2(r;N_t) = h_2(r,r_n;D_0) - 2\int_r^{r_n} N_t(s) f_2(s;D_0,\mu) ds \tag{17}$$

with

$$\begin{aligned} g_1 &= \delta I_b(r) \\ h_1 &= \delta(\widetilde{Z}_m(r) + A_r(r_n)) + \delta(A_c(r) + A_v(r)) \\ f_1 &= \delta I_e(r) \end{aligned} \tag{18}$$

$$\begin{aligned} g_2 &= 10\log_{10} N_t(r) \\ h_2 &= \widetilde{Z}_m(r) + A_r(r_n) - I_b(r) + (A_c(r) + A_v(r)) \\ f_2 &= I_e(r) \end{aligned}$$

where δ is a difference operator, defined in the case of dual-polarization radar by $\delta X \equiv \delta_p X \equiv X_{hh} - X_{vv}$ and in the case of a dual-frequency radar by $\delta X \equiv \delta_f X \equiv X(f_1) - X(f_2)$. Note that in the case of the polarimetric radar, $\delta(A_c + A_v) = 0.$ Using the definition of I_b given by (9), the usual differential reflectivity (in dB) with respect to polarization is $\delta I_b = Z_{dr}$ while the dual-frequency ratio (in dB) is $\delta I_b = DFR$.

The constraints in the above equations are assumed to be the precipitation path attenuations at the 2 frequencies or 2 polarizations. If the constraint is total path attenuation from precipitation, cloud and water vapor, then h_1, h_2 should be changed to:

$$\begin{aligned} h_1 &= \delta(\widetilde{Z}_m + A(r_n)) - \delta(A_c(r,r_n) + A_v(r,r_n)) \\ h_2 &= \widetilde{Z}_m + A(r_n) - I_b - (A_c(r,r_n) + A_v(r,r_n)) \end{aligned} \tag{19}$$

where, as before,

$$A(r_n) = A_r(r_n) + A_c(r_n) + A_v(r_n) \tag{20}$$

The two forms for h_1 and h_2 in (18) and (19) are identical. However, if an independent estimate is made of the precipitation attenuation only, $A_r(r_n)$, then contributions from cloud water and water vapor to range r must be added in, as in (18). If an independent estimate is made of total attenuation, then contributions from cloud water and water vapor over the range interval (r, r_n) must be subtracted out, as in (19). To simplify the equations, we assume for the remainder of the paper that attenuation from cloud and water vapor can be neglected.

If the path attenuation is known or assumed, then from (16) and (17) it can be seen that the range profiles of D_0 and N_t can be obtained by starting at the far range, r_n, continuing inward towards the radar. At $r = r_n$, the integrals appearing in (16) and (17) are zero so that D_0 can be found by numerically solving the equation $g_1(D_0,\mu) = h_1$; once D_0 is determined, it is substituted into (17) to give N_t. Proceeding to the $(n-1)^{th}$ gate, the values of D_0 and N_t from the nth gate are substituted into the integrals in (16) and (17); since the right-hand side of (16) is determined, D_0 can be solved numerically. Substituting this into (17) gives h_2 and N_t. The recursion continues in this way until the full path is traversed.

In solving the equations numerically, the discrete forms of (16) and (17) take the form of non-linear algebraic equations for D_0 and N_t that can be solved by Broyden's method [Press et al., 1992]. For example, at the final gate, both (16) and (17) are functions of $D_0(r_n)$ and $N_t(r_n)$ if the contributions from the last gate are included. However, if the attenuation per range gate is small, the approximate and general procedures yield nearly identical results. It should also be pointed out that in some cases, such as the dual-wavelength radar returns in rain or mixed-phase hydrometeors, there can be more than one value of D_0 that satisfies (16). Procedures exist to reduce the ambiguities but not eliminate them entirely [Liao and Meneghini, 2005]. Note also that as there are only two equations, the 'shape' parameter μ must either be fixed or expressed as a function of the other DSD parameters [Zhang et al., 2001; Seifert, 2005].

As pointed out by Mardiana et al. (2004), consistency requires that the estimated parameters of the size distribution give back the path-integrated attenuations used in the integral equations. In other words, the input and output path attenuations must be equal. Although this condition was originally imposed for the unconstrained solution, it can be applied generally since there exist other parameters that can be adjusted even in the constrained case. Let

$(\hat{N}_t(r,\mu), \hat{D}_0(r,\mu))$ represent the range profiles of the particle number concentration and median mass diameter obtained from (16) and (17). As these values depend on the value of μ used in (16) and (17), they have been written explicitly with this dependence. Then the estimated path attenuations can be written:

$$\hat{A}_{pp}(r_n, f_i; \mu) = c_e \int_{s=0}^{r_n} \hat{N}_t(s,\mu) \int_0^{\infty} \sigma_{e,pp}(f_i, D) n(D; \hat{D}_0(s,\mu)) dD ds \quad (21)$$

Eq. (21) represents two path attenuations either for two polarizations at a fixed frequency or two frequencies at a fixed polarization. If we let $A_{pp}(r_n, f_i; \mu)$ represent the input values to (16) and (17), then the objective is to obtain agreement between the input and output values:

$$\hat{A}_{pp}(r_n, f_i; \mu) \leftrightarrow A_{pp}(r_n, f_i; \mu) \quad (22)$$

If independent estimates of the PIA values are not available, the values used in the (16) and (17) are initial guesses (e.g., both zero). In this case, it is reasonable to compute the DSD parameters from (16) and (17) then use (21) to update the PIA values and to continue the procedure until consistency is attained. This is essentially the iterative procedure of Mardiana et al. (2004). On the other hand, if the path attenuations are estimated from independent data, then it is possible to iterate on other parameters. For example, a possible way of obtaining consistency is to modify the assumed value of μ until $\hat{A}_{pp}(r_n, f_i; \mu) \approx A_{pp}(r_n, f_i; \mu)$. In cases where mixed-phase particles are present along the beam or if cloud water and water vapor attenuation are not negligible, then a larger set of variables would be available for adjustment to satisfy the consistency condition. Clearly, as the number of potential adjustment parameters increase, the 'dimensionality' of the ambiguity will also increase so that, potentially, many sets of such parameters will approximately satisfy (22). Another possibility, however, is that adjustment of certain parameters leave the input and output path attenuations unchanged so that consistency condition provides no additional information. Finally, it is worth noting that in the unconstrained case, it is not possible to optimize over any other parameter because the consistency conditions are used to obtain the path attenuations.

3. SIMULATION RESULTS

To illustrate some aspects of the solutions to the integral equations, we construct a simulation for an X-band polarimetric radar using disdrometer-measured raindrop size distributions. For the cases shown, we have assumed a 50-km path consisting of 250 gates with range resolution 0.2 km. A sequence of 250 30 s-averaged drop size distributions provide the particle number concentration and median mass diameter at each range gate. Assuming the Beard and Chuang [1987] shape-size relationship and a fixed μ value along the path, the simulated range profiles at the two polarizations are calculated, i.e., $\{Z_{m,hh}(r_j), Z_{m,vv}(r_j)\}; j = 1,..,n$ where $n = 250$. To simplify the discussion, we assume that the data are unbiased and without fluctuations from finite sampling. We also assume either that the values of the path attenuation are known and equal to the true value (constrained) or they are not known (unconstrained). In the latter case, iteration is performed. The iteration begins with the assumption that the path attenuations at the two polarizations are zero and finishes when the input and output path attenuations in (22) agree to within a certain tolerance. However, if the difference between input and output path attenuations increases at any stage, the iteration is terminated.

In Fig. 1, the black curves represent the range profiles of rain rate, median mass diameter and number concentration as derived from the raindrop size distributions along the path. Retrieved values of these same parameters for the constrained and unconstrained solutions to (16) and (17) are shown by the red and blue curves, respectively. In this relatively light rain rate case

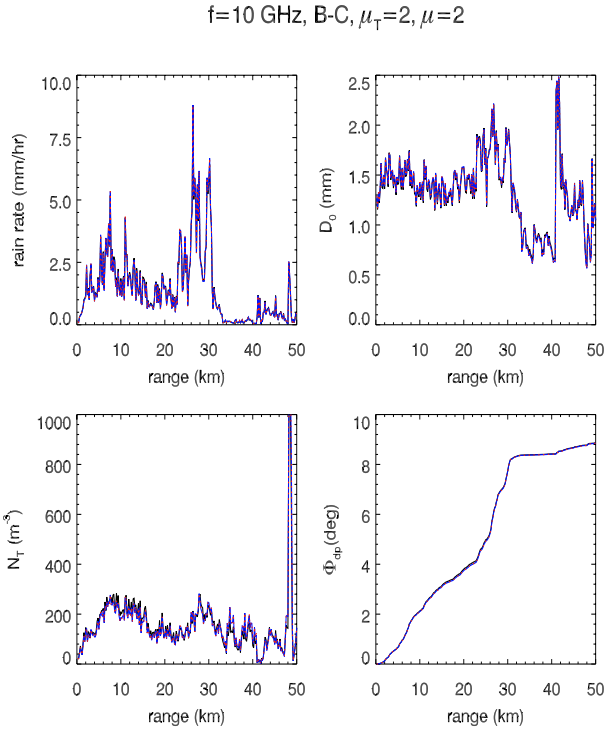

Fig. 1. Comparisons of the assumed or 'true' (black), with the iterative (blue) and constrained (red) estimates for rain rate, median mass diameter, D_0, and particle number concentration, N_t, for a light rain rate case. In the lower right panel, the true differential phase is compared with values of the differential phase calculated from the DSD parameters derived from the iterative (blue) and constrained (red) retrievals.

and at the 'mildly' attenuated frequency of 10 GHz, the results from the two approaches are nearly identical and nearly indistinguishable from the true values. The results Ilustrate an important property of the iterative solution: in cases where the path attenuation is small, stable solutions can be obtained without a path-attenuation constraint. As a check of the results, we show in the lower right panel, the true differential phase compared with values of the differential phase calculated from the DSD parameters derived from the iterative (blue) and constrained (red) retrievals.

A second case with higher rain rates along the path is shown in Fig. 2. For this profile, the iteration shows some instabilities (blue curves) where the rain rates and number concentrations tend to be positively biased while the median mass diameter tends to be negatively biased. On the other hand, the range profiles of the various quantities using the PIA constraints remain nearly identical to the true profiles. In Figs. 1 and 2 the value of μ used to generate the simulated data is the same as that used in the retrieval: $\mu = \mu_T = 2$. For the results in Figs. 3 and 4, we have kept the simulated data data the same as in Fig. 2 ($\mu_T = 2$) but have changed the value of μ used in the retrieval: for Fig. 3, $\mu = 0$ and for Fig. 4, $\mu = 6$. Inspection of the results show that for $\mu < \mu_T$ the constrained and unconstrained methods overestimate the rain rate and number concentration

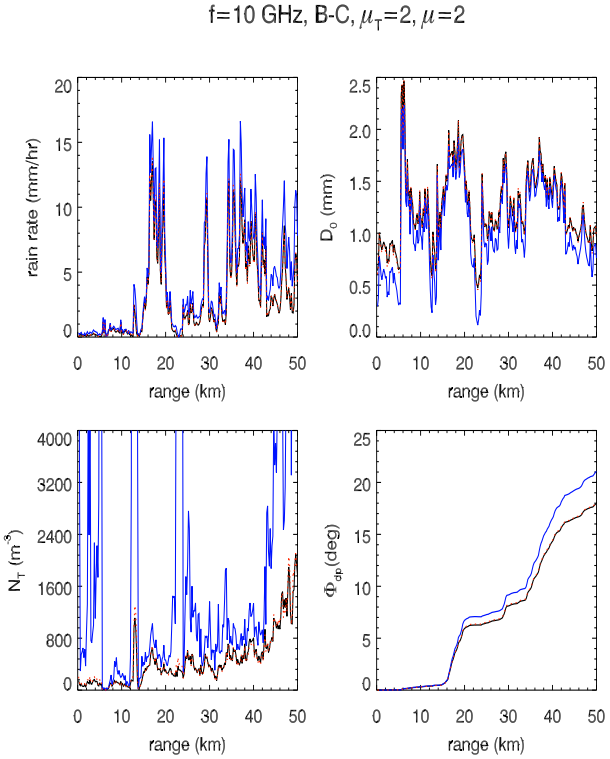

Fig. 2. Same as Fig. 1 but for a moderate rain rate case.

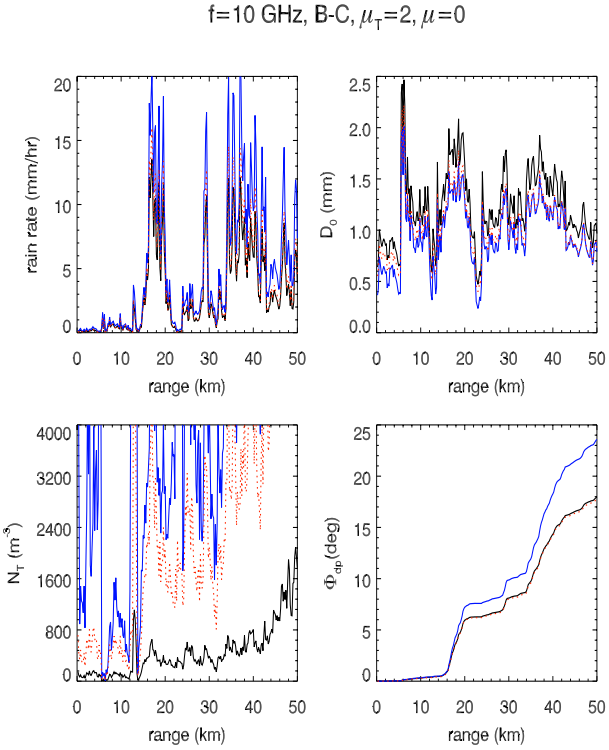

Fig. 3. Same as Fig. 2 but for $\mu_T = 2, \mu = 0$.

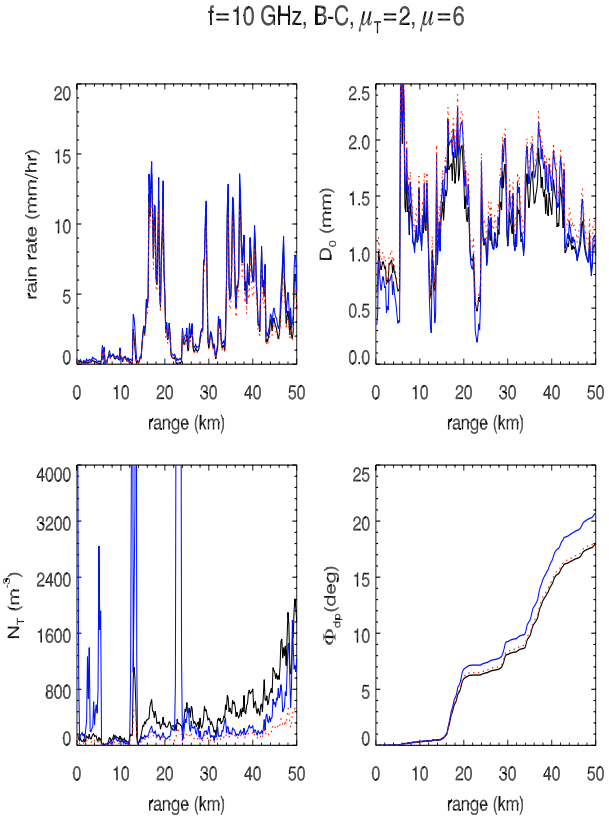

Fig. 4. Same as Fig. 2 but $\mu_T = 2, \mu = 6$.

and underestimate the median mass diameter. For $\mu < \mu_T$, the opposite behavior is generally seen apart from occasional instabilities in the unconstrained profiles.

It is worth noting that a search over the constrained solutions for the best μ value is ineffective in these cases because the output path attenuation is nearly independent of μ. This can be seen in the comparisons of the true and retrieved values of Φ_{dp} in Figs. 2 through 4 which show that the DSD parameters from the constrained solution (red curves) are able to reproduce accurately the true Φ_{dp} profile (black curve) in all cases. In other words, even when μ is incorrect, the estimated DSD parameters yield approximately the same path attenuation and same Φ_{dp} profile. It is also worth noting that while the integral equations given here have number concentration and median mass diameter as the unknowns, they also can be written using the parameters of the "normalized" size distribution [Testud et al., 2001]. Whether this would lead to smaller variations in the rain rate estimates with changes in μ is an open question.

4. COMPARISON WITH AN ALTERNATIVE METHOD

Testud et al. (2000) and Bringi et al. (2001) recognized that techniques developed for single attenuating-wavelength radars can be applied to polarimetric radar data at attenuating wavelengths. Although a detailed comparison of this type of method with that given here is beyond the scope of the paper, it is worth pointing out some similarities and differences. These methods are a subset of a larger class of polarimetric attenuation correction methods reviewed by Bringi and Chandrasekar (2001). Extensions of the basic approach have been proposed as well, e.g., Lim and Chandrasekar (2005).

Although most formulations begin with the final-value solution of Marzoug and Amayenc (1991, 1994), an equivalent form follows directly from the 'α-adjustment' solution [Meneghini et al., 1983; Iguchi and Meneghini, 1994] where, taking $10\log_{10}$ of (19) of Iguchi and Meneghini, and assuming that the coefficient α in the k-Z relationship is constant, gives ($r \le r_n$):

$$\widetilde{Z}(r) = \widetilde{Z}_m(r) - \beta^{-1} 10 \log_{10} Q \tag{23}$$

where

$$Q = 1 + (10^{-0.1\beta A(r_n)} - 1)(S(r)/S(r_n)) \tag{24}$$

$$S(r) = \int_0^r Z_m^{\beta}(s)ds \tag{25}$$

$$k = \alpha Z^{\beta} \tag{26}$$

It is worth noting that (23) also holds if α varies with range (e.g., both stratiform and convective rain are present along the path or the path contains separate regions of frozen, mixed phase and liquid precipitation). In this case, however, S must be replaced with the original definition:

$$S(r) = \int_0^r \alpha(s) Z_m^{\beta}(s)ds \tag{27}$$

For constant α along the path, Eq. (23) can also be obtained by taking the expression for k from the final-value solution ((24) of Testud et al. (2000)), integrating it from 0 to r and using the definition of Z_m:

$$\widetilde{Z}(r) = \widetilde{Z}_m(r) + 2\int_0^r k(s)ds \tag{28}$$

For polarimetric applications, the 2-way path attenuation, $A(r_n)$, can be expressed as a function of the differential phase shift over the path, $\Delta\Phi_{dp}$, by using a relationship between k and κ_{dp} [Testud et al., 2000]. In the case of a linear k-κ_{dp} relationship:

$$k_{pp} = \gamma_{pp}\kappa_{dp} \tag{29}$$

then,

$$A_{pp}(r_n) = 2\int_0^{r_n} k_{pp}(s)ds = 2\gamma_{pp}\int_0^{r_n} \kappa_{dp}(s)ds = \gamma_{pp}\Delta\Phi_{dp} \tag{30}$$

To compare with the results given previously, we will use the 2-way path attenuation, $A(r_n)$, instead of $\Delta\Phi_{dp}$.

It is first convenient to write Q in (24) as:

$$Q = 10^{-0.1\beta A(r_n)}[10^{0.1\beta A(r_n)} + (1 - 10^{0.1\beta A(r_n)})(S(r)/S(r_n))] \tag{31}$$

so that (23) becomes

$$\widetilde{Z}(r) = \widetilde{Z}_m(r) + A(r_n) - \beta^{-1} 10 \log_{10} \widetilde{Q} \tag{32}$$

where

$$\widetilde{Q} = 10^{0.1\beta A(r_n)} + (1 - 10^{0.1\beta A(r_n)})(S(r)/S(r_n)) \tag{33}$$

Using (32), equations analogous to (12) and (13) can be obtained, as before, by expressing $\widetilde{Z}_{m,pp}(r,f)$ and $\widetilde{Z}_{m,hh}(r,f)-\widetilde{Z}_{m,vv}(r,f)$ in terms of D_0 and N_t:

$$I_{b,hh}(r)-I_{b,vv}(r)=(\widetilde{Z}_{m,hh}(r)-\widetilde{Z}_{m,vv}(r))+ \\ +(A_{hh}(r_n)-A_{vv}(r_n))-\beta^{-1}10\log_{10}(\widetilde{Q}_{hh}/\widetilde{Q}_{vv}) \quad (34)$$

$$\widetilde{N}_t(r)=\widetilde{Z}_m(r)-I_b(r)+A(r_n)-\beta^{-1}10\log_{10}\widetilde{Q} \quad (35)$$

where, as before,

$$\widetilde{N}_t \equiv 10\log_{10} N_t \quad (14)$$

Also, as before, we have suppressed the subscripts in (35) since all relevant quantities are evaluated at the same polarization. Other quantities in (34) and (35) are defined above but without subscripts. Explicitly:

$$\widetilde{Q}_{pp}=10^{0.1\beta A_{pp}(r_n)}+(1-10^{0.1\beta A_{pp}(r_n)})(S_{pp}(r)/S_{pp}(r_n)) \quad (36)$$

$$S_{pp}(r)=\int_0^r \alpha_{pp}(s)Z_{m,pp}^{\beta}(s)ds \quad (37)$$

In (37) we have used the more general definition of S; however, if α is assumed constant then because S appears only in a ratio, the α dependence is eliminated.

Comparisons of (12) and (13) with (34) and (35) (and neglecting attenuation from cloud and water vapor as these contributions are not included in (34) and (35)) show that the only differences between the two sets of equations are the terms:

$$2\int_r^{r_n} N_t(s)I_e(s)ds \leftrightarrow \beta^{-1}10\log_{10}\widetilde{Q} \quad (38)$$

$$2\int_r^{r_n} N_t(s)[I_{e,hh}(s)-I_{e,vv}(s)]ds \leftrightarrow \beta^{-1}10\log_{10}(\widetilde{Q}_{hh}/\widetilde{Q}_{vv})$$

The right and left-hand sides of (38) represent the different ways that the algorithms account for the attenuation and differential attenuation in the range interval from r to r_n. In the integral equation approach, the interval attenuations are expressed as functions of the DSD parameters obtained from previous steps in the recursion. In the single-wavelength approach, the attenuations are estimated by means of the k-Z parameterization. In both cases, these contributions are subtracted from the total path attenuation to obtain an estimate of attenuation to range r. Note that in the single-wavelength algorithm, upon which (34) and (35) are based, profiles of a 2-parameter DSD can not be obtained from a single path-attenuation constraint.

How this basic difference translates into differences in performance is difficult to assess without a detailed error analysis. A few obvious differences can be pointed out, however. The single-wavelength approach relies on the parameters of the k-Z relationship, although for constant α, the estimate is independent of this parameter. The integral equations are independent of the k-Z relationship. On the other hand, if the DSD parameterization depends on more than 2 parameters, an assumption regarding the third parameter must be made. Figs. 3 and 4 show that errors in μ can produce significant errors in the estimates; moreover, the consistency condition in this case does not help to identify the correct value because the DSD parameters that are produced under the different μ assumptions all yield approximately self-consistent results.

Another difference between the two approaches is that the single-wavelength constraints used in (34) and (35) seem to require estimates of the path attenuation at the two polarizations. Although the integral equations were originally formulated to be used with the same type of constraints, Mardiana et al. (2004) have shown that this is not required. (Whether a similar property holds for (34) and (35) is an open question.) In practice, however, it appears that the iteration converges only when the path attenuation is not too large. In fact, even when accurate path attenuations are used as constraints, it is not difficult to find rain rate profiles in which both formulations fail to converge over the full path. The k-Z parameterization used in (34) and (35) does not depend on the explicit DSD retrievals in the range from r to r_n; as a consequence, these equations may be more robust than are the integral equations. Clearly, however, a detailed error analysis is needed before the relative advantages of the various formulations can be assessed.

5. SUMMARY AND CONCLUSIONS

Integral equations for the parameters of the particle size distribution have several useful features in that they explicitly include path attenuation constraints and provide attenuation correction in terms of the particle size distribution parameters in the far range gates. Because the dual-wavelength and dual-polarization radar are governed by essentially the same equations, a common theoretical framework is provided by which errors in the retrievals can be assessed. This may be of some benefit to the proposed Global Precipitation Measurement Mission [Iguchi et al., 2002] where quantities derived from a dual-wavelength spaceborne radar can be expected to be compared with similar quantities derived from ground-based dual-polarization radars. Making good use of these data will depend on

an understanding of the inherent errors in both spaceborne and ground-based algorithms.

It is worth noting that apart from the integral equation approach, many dual-wavelength techniques have been proposed [e.g., Marzoug and Amayenc, 1994; Adhikari and Nakamura, 2003; Grecu and Anagnostou, 2004]. In view of the close relationship between dual-wavelength and dual-polarization algorithms, these formulations may also be applicable to dual-polarization data at attenuating wavelengths.

Although the integral equation approach has been used to analyze airborne dual-wavelength data, its utility for dual-polarization applications at an attenuating-wavelength has not been assessed. This work, along with comparisons to existing attenuation correction methods, is needed to demonstrate that the formulation is useful for practical applications.

REFERENCES

Adhikari, N.B. and K. Nakamura, 2003: Simulation-based analysis of rainrate estimation errors in dual-wavelength precipitation radar from space. *Radio Sci*., **38**, No. 4, Art. No. 1066.

Beard, K.V. and C. Chuang, 1987: A new model for the equilibrium shape of raindrops. *J. Atmos. Sci*., **44**, 1509-1524.

Bringi, V.N., T.D. Keenan and V. Chandrasekar, 2001: Correcting C-band radar reflectivity and differential reflectivity data for rain attenuation: a self-consistent method with constraints. *IEEE Trans. Geosci. Remote Sens*., **39**, 1906-1915.

Bringi, V.N. and V. Chandrasekar, 2001: *Polarimetric Doppler Weather Radar: Principles and Applications*. Cambridge University Press, New York, NY.

Grecu, M. and E.N. Anagnostou, 2004: A differential attenuation based algorithm for estimating precipitation from dual-wavelength spaceborne radar. *Can. J. Remote Sens*., **30**, 697-705.

Hitschfeld, W. and J. Bordan, 1954: Errors inherent in the radar measurement of rainfall at attenuating wavelengths. *J. Meteor*., **11**, 58-67.

Iguchi, T. and R. Meneghini, 1994: Intercomparison of single-frequency methods for retrieving a vertical rain profile from airborne or spaceborne radar data. *J. Atmos. Oceanic Technol*., **11**, 1507-1516.

Iguchi, T., R. Oki, E.A. Smith and Y. Furuhama, 2002: Global Precipitation Measurement program and the development of dual-frequency precipitation radar. *J. Comm. Res. Lab. (Japan)*, **49**, 37-45.

Lim. S. and V. Chandrasekar, 2005: A dual polarization rain profiling algorithm. *IEEE Trans. Geosci. Remote Sens*., (submitted).

Liao L. and R. Meneghini, 2005: A study of air/space-borne dual-wavelength radar for estimates of rain profiles. *Adv. Atmos. Sci*. (in press).

Mardiana, R., T. Iguchi, and N. Takahashi, 2004: A dual-frequency rain profiling algorithm without the use of the surface reference technique. *IEEE Trans. Geosci. Remote Sens*., **42**, 2214-2225.

Marzoug. M. and P. Amayenc, 1991: Improved range-profiling algorithm of rainfall rate from a spaceborne radar with path-integrated attenuation constraint. *IEEE Trans. Geosci. Remote Sens*., **29**, 584-592.

Marzoug, M. and P. Amayenc, 1994: A class of single- and dual-frequency algorithms for rain-rate profiling from a spaceborne radar. Principle and tests from numerical simulations. *J. Atmos. Oceanic Technol*., **11**, 1480-1506.

Meneghini, R., J. Eckerman, and D. Atlas, 1983: Determination of rain rate from a space-borne radar using measurements of total attenuation. *IEEE Trans. Geosci. Remote Sens*., **21**, 34-43.

Meneghini, R., T. Kozu, H. Kumagai, and W.C. Boncyk, 1992: A study of rain estimation methods from space using dual-wavelength radar measurements at near-nadir incidence over ocean. *J. Atmos. Oceanic Technol*., **9**, 364-382.

Press, W.H., S.A. Teukolsky, W. T. Vetterling, and B.P. Flannery, 1992: *Numerical Recipes in FORTRAN, 2nd Edition*, Cambridge University Press. 933 pp.

Seifert, A., 2005: On the shape-size relation of drop size distributions in convective rain. *J. Appl. Meteor*., 44, 1146-1151.

Testud. J., E. Le Bouar, E. Obligis, and M. Ali-Mehenni, 2000: The rain profiling algorithm applied to polarimetric weather radar. *J. Atmos. Oceanic Technol*., **17**, 332-356.

Testud. J., J. Oury, R.A. Black, P. Amayenc, and X. Dou, 2001: The concept of "normalized" distribution to describe raindrop spectra: a tool for cloud physics and cloud remote sensing. *J. Appl. Meteor.,* **40**, 1118-1140.

Zhang, G., J. Vivekanandan, and E. Brandes, 2001: A method for estimating rain rate and drop size distribution from polarimetric radar measurements. *IEEE Trans. Geosci. Remote Sens.,* **39**, 830-841.